Building and Environment 288 (2026) 113934

Contents lists available at ScienceDirect

Building and Environment

journal homepage: www.elsevier.com/locate/buildenv

Emission of airborne particles from 3D printing using thermoplastic polymeric materials

L. Fappiano [a], E. Caracci [a,*], A. Ceccacci [a], G. Iannitti [a], G. Buonanno [a,b], L. Stabile [a]

[a] Department of Civil and Mechanical Engineering, University of Cassino and Southern Lazio, Cassino, FR, Italy
[b] International Laboratory for Air Quality and Health, Queensland University of Technology, Brisbane, Qld, Australia

ARTICLE INFO

Keywords:
3D printing
Ultrafine particles
Particle number distribution
Fused deposition modeling
Emission rate

ABSTRACT

3D printing activities are recognized to emit airborne particles. Several papers in scientific literature quantified the particle emission for different filament materials; nonetheless, a knowledge gap still exists for some advanced materials. To this end, we evaluated the particle emissions from a 3D printer using thermoplastic polymeric materials, including thermoplastic elastomer (TPE), thermoplastic polyurethane (TPU), thermoplastic polyurethane enhanced with carbon nanotubes (TPU-CNT), polycarbonate (PC), and polypropylene (PP). Data for various printing temperatures and printing chamber configurations (open and closed with a HEPA filter) were provided.

For all the investigated materials and temperatures, negligible emissions in terms of PM were recognized. Particle number emission rates with the chamber closed were one order of magnitude lower than those for tests with the chamber open. A temperature effect was also detected; higher emission rates and lower particle distribution modes were estimated for higher extrusion temperatures. Amongst the tested materials, PP and PC filaments presented the highest emission factors (up to 1×10^{12} part. min^{-1} for open printing chamber).

The obtained emission rates were adopted to estimate the average particle number concentration in a real-world scenario when performing 3D printing activities: in a 40 m^3 office, when printing chambers with HEPA filters are adopted, the 1-hour average concentration is lower than the WHO guideline value, regardless of the filament and the air exchange rates. On the contrary, without a printing chamber, the WHO guideline values are only met with less emitting filaments and high ventilation rates.

1. Introduction

Exposure to airborne particles in indoor environments poses a considerable concern for human health [1], as indoor particle sources lead to considerably high concentrations [2,3]. The principal sources of particles in indoor environments include cooking activities, the burning of incense or candles, and the use of mosquito coils; additionally, resuspension of particles can occur from everyday movements or cleaning activities [2,4–19], along with secondary particles formed from chemical reactions in the air [20,21]. Even in clean indoor environments (non-smoking spaces), unexpected sources of particles, such as printers and photocopiers, can be present; these devices are significant emitters of ultrafine particles [22–24].

1.1. 3D printing as a source of airborne particles

In recent years, the adoption of 3D printers has become increasingly common among the population, leading to greater use in homes and work settings. According to Google Trends, interest in 3D printers has risen during 2024, driven primarily by decreasing prices and growing accessibility. Among the various 3D printing technologies, fused deposition modeling (FDM) and stereolithography (SLA) are the primary methods. Of these, FDM remains the most popular due to its lower printer costs, the affordability of filaments compared to resins, and user-friendly operation [25]. Furthermore, FDM-printed objects typically require minimal to no post-processing, simplifying the overall production workflow. These characteristics made FDM printers widespread not only in industries, but also in private houses, schools, and environments not intended to host manufacturing systems and often unsuitable for treating fumes from these devices [26]. Moreover, the range of available

* Corresponding author at: Department of Civil and Mechanical Engineering, University of Cassino and Southern Lazio, Cassino, FR, Italy.
E-mail address: elisa.caracci@unicas.it (E. Caracci).

https://doi.org/10.1016/j.buildenv.2025.113934
Received 23 June 2025; Received in revised form 29 October 2025; Accepted 30 October 2025
Available online 30 October 2025

filaments for FDM is continually expanding, now including advanced materials such as thermoplastic polymeric materials (e.g., thermoplastic polyurethane, thermoplastic elastomer, polypropylene, polycarbonate, etc.), raising concerns among users regarding potential emissions from these devices. The majority of the existing literature on airborne particle emission from FDM 3D printing has predominantly focused on acrylonitrile butadiene styrene (ABS) and polylactic acid (PLA) based filaments [27–44]. However, several studies have also investigated a broader range of materials, including Nylon, various PLA formulations, polyethylene terephthalate (PET), polyethylene terephthalate glycol (PETG), PP, TPU, high impact polystyrene (HIPS), polyvinyl alcohol (PVA), T-glase, and PCABS [39,45–53]. Most studies rely on similar instruments, including particle counters (condensation particle counters, optical particle counters, photometers, …) and particle sizers (Differential Mobility Particle Sizer).

1.2. Quantifying the airborne particle emission from 3D printers

Most of the studies primarily report on the particle concentration ranges and size distributions of various filaments, but do not provide data on emission rates. This emission rate data is essential for quantifying the particle emissions from different sources and estimating exposure levels in various indoor scenarios (e.g., adopting well-mixed models). This significant gap in data availability does not allow for a complete comprehension and evaluation of the human health risks associated with 3D printing in indoor environments, such as homes and offices. Therefore, assessing the emissions linked to these materials before their market introduction is imperative. This approach will not only enhance the awareness of the health risks associated with 3D printing but also support the development of safer practices and regulations in this rapidly evolving field. In a previous study, we examined the emission rates of different printing materials [52], showing the effect of the type of filament on the emission rates and the impact of the printing temperature. Indeed, we showed that different filament materials can produce different particle emission rates.

1.3. Aims of the work

In the present study, we estimated the particle emission rates and the particle size distributions during the FDM printing process when using thermoplastic polymeric materials. We also evaluated the effect of printing temperature on particle emission. Indeed, printing processes with different materials (thermoplastic polyurethane, thermoplastic polyurethane enhanced with carbon nanotubes, thermoplastic elastomer, polypropylene, and polycarbonate) and printing temperatures (ranging in a temperature interval close to the suggested printing temperature) were performed through a commercially available 3D printer.

2. Materials and methods

2.1. Sampling site and experimental apparatus description

Measurements were carried out at the Laboratory of Industrial Measurements (LAMI) of the University of Cassino and Southern Lazio, Italy, where the HVAC system guarantees constant temperature and relative humidity, i.e., 20 °C and 50 %, respectively. Tests were performed in a 1.80 m × 1.20 m × 2.20 m plexiglass chamber (hereafter referred to as the measurement chamber) presenting a small opening allowing air supply for electrical cables and ducts. The air exchange rate of the chamber in this condition was measured adopting a CO_2 decay method [54] and resulted in 0.50 ± 0.03 h^{-1}. The instruments used for characterizing the emissions of various filaments utilized in 3D printing are CPC, SMPS, and DustTrak. The CPC (CPC 3775, TSI Inc.) is a butanol-based Condensation Particle Counter; this instrument measures the particle number concentration of particles greater than 4 nm in diameter, with a maximum capability of measuring up to 10^7 part. cm^{-3} using a 1-second sampling time. The SMPS (SMPS 3936, TSI Inc.) is a Scanning Mobility Particle Sizer Spectrometer, this device measures the particle number distribution in the sub-micrometric range: it comprises an Electrostatic Classifier (EC 3080, TSI Inc.), which classifies particles according to their electrical mobility diameter, and a further CPC 3775 that counts the classified particles, thereby providing particle number size distribution. In the experimental analysis, a sampling time of 135 s, an aerosol flow rate of 1.5 L min^{-1}, and a sheath flow rate of 15 L min^{-1} were utilized, resulting in particle size distributions within the 6–220 nm mobility diameter range. The DustTrak (DustTrak aerosol monitor 8534, TSI Inc.) is a light-scattering laser photometer that can measure particle mass concentrations in terms of PM_1, $PM_{2.5}$, and PM_{10}, with a sampling time of 1 s. Temperature and relative humidity were also measured during the tests through an Aranet4 Pro air quality monitor, which possesses the capability to assess temperature and relative humidity with a 1-minute sampling frequency.

2.2. Emission sources: printer and filaments

The evaluation of particle emission was conducted on various filaments, all of which are part of the family of thermoplastic polymeric materials. Specifically, five materials were studied: thermoplastic polyurethane (TPU), thermoplastic polyurethane enhanced with carbon nanotubes (TPU-CNT), thermoplastic elastomer (TPE), polypropylene (PP), and polycarbonate (PC). All the filaments used were selected from commercially available options. These thermoplastic materials have numerous applications, including sealing, insulation, shock-absorbing protection, packaging, and more. The characteristics of thermoplastic polymers vary depending on the type. Still, they are generally recognized for their lightweight, ability to sustain high deformations and dissipate energy under dynamic loads, as well as their durability, high recyclability, and reduced cost [55–59].

The 3D printer employed in this study was the Pro II, manufactured by ZYYX 3D, a tabletop FDM printer with the characteristics reported in Table 1. The device is equipped with a printing chamber that can be either closed or open. A filtering system is also integrated within the printer, consisting of a combined HEPA H13 and active carbon filter, fed by a ventilation fan.

The printing process was set up using Simplify 3D software; the main process parameters are reported in Table 2. Before printing, the printing chamber was preheated, and measurements were conducted in both open and closed configurations to simulate the emissions of printers with and without printing chambers. Before each test, the printer underwent a pre-heating phase, enabling the chamber to reach the target temperature (40 °C). The automatic bed level calibration, nozzle heating, and a spot-print for nozzle purge followed the pre-heating phase. Before printing the sample, a brim was printed around the object (a common practice with the primary purpose of stabilizing the filament flow through the nozzle).

Table 3 shows detailed properties of the filaments used in the study. The table includes the characteristics along with additional relevant information.

The object printed, reported in Fig. 1, was a parallelepiped (width=10 mm, depth=10 mm, height=5 mm). Stefaniak et al. [60] report that the filament color can influence the particulate emission;

Table 1
Technical specification of the printer.

Print technology	Fused Deposition Modelling (FDM)
Build volume	285 × 235 × 210 mm
Printing (extruder) temperature	100–275 °C
Chamber temperature	Up to 75 °C
Print Speed	Up to 200 mm s^{-1}
Max resolution	50 μm layer thickness, 11 μm XY positioning
Filament feed system	Direct drive (1.75 mm filament)
Nozzle diameter used	0.6 mm

Table 2
Main printing process parameters.

Chamber temperature	40 °C
Layer thickness	0.2 mm
Average print speed	400 mm min^{-1}
Infill	100 %
Infill pattern	Rectilinear
Nozzle temperature	220, 230, 240 °C for TPE, TPU, TPU-CNT, PP; 235, 245, 255 °C for PC

Table 3
Detailed properties of the filaments used in the study.

	TPE	TPU	TPU-CNT	PP	PC
Manufacturer	ESun	Geeetech	Essentium (Nexa3D)	CC3D	Eono
Additives	–	–	Carbon Nanotubes 0.01 %	–	–
Diameter (mm)	1.75	1.75	1.75	1.75	1.75
Color	White	Black	Black	Black	Black
Density (g cm^{-3})	1.14	1.2	1.23	0.95	1.2
Hardness	83A	95A	74D	–	–
Melting temperature (°C)	175–195	190–200	190–200	130–160	220–230
Glass transition temperature (°C)	−50 – −60	−16 – −30	−35	−20	107–150

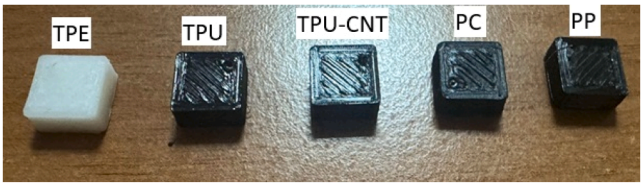

Fig. 1. Printed parallelepipeds with the different filaments under testing: thermoplastic elastomer (TPE), thermoplastic polyurethane (TPU), thermoplastic polyurethane enhanced with carbon nanotubes (TPU-CNT), polycarbonate (PC), and polypropylene (PP).

thus, the colors of all filaments utilized in the present work were black, except for the TPE, which was white. The nozzle temperature was adjusted according to the manufacturer's guidelines, set at 230 °C for TPE, TPU, TPU-CNT, and PP, and 245 °C for PC. To evaluate the impact of extrusion temperature on emissions during the printing process, two additional tests were conducted for each material at ±10 °C, corresponding to the suggested printing temperature. The heating chamber temperature remained consistent throughout all tests during the printing process.

2.3. Methodology

The 3D printer was placed in the center of the measurement chamber, and all the instruments described in Section 2.1 were positioned inside the chamber at approximately 20 cm from the printing chamber, thus avoiding extension tubes and minimizing potential particle losses in ducts.

The measurement procedure adopted consisted of: (i) 10 min of background measurements during which the printer heated the printing chamber, (ii) measurement during the printing process of the parallelepiped, with a duration of about 10 min independently of the filament material used, (iii) the measurement during the particle concentration decay occurring after the printing process. From the concentration trends obtained from the CPC, the emission rate (ER) has been estimated using a well-known mass-balance equation derived by He et al. [61]:

$$ER = V \cdot \left[\frac{C_{in,peak} - C_{in,0}}{\Delta t} + (\overline{AER + k}) \cdot C_{in} - AER \cdot C_{in,0} \right] \quad (1)$$

where $C_{in,peak}$ and $C_{in,0}$ represent the peak and the initial (i.e., background) particle concentrations, C_{in} is the average concentration in the measurement chamber during the test, AER is the air exchange rate (reported in the Section 2.1), k is the deposition rate, $\overline{AER + k}$ is the average total removal rate (calculated from the decay rate of particle concentration after the emission activity ceased), Δt is the time difference between initial and peak concentrations, V is the volume of the measurement chamber. This equation can be applied when particle condensation, evaporation, and coagulation effects are negligible [61]. For more information regarding the ER evaluation, readers are directed to our previous papers [2,4,52]. A test was conducted for each filament at each extrusion temperature with the printing chamber open. A further test was also performed with the printing chamber closed for the optimal temperatures for printing (230 °C and 245 °C).

To assess the repeatability of the test, five measurements were conducted for each test condition (i.e., different temperatures, filaments, and printing chamber conditions). We note that each measurement was performed as an independent printing activity (i.e., it is not a repeated measurement under the same emission episode).

A statistical analysis was performed to determine whether the estimated emission rates as a function of the filament and the extrusion temperature were statistically different. Thus, a preliminary normality test (Shapiro-Wilk test) was performed to check the statistical distribution of the data. Since the data met a Gaussian distribution, a parametric test (ANOVA test) and a further post-hoc test (Tukey-Kramer test) [62] were considered in the analysis. A confidence level of 95 % was adopted (significance level of $p = 0.05$).

2.4. Exposure in a real-world scenario

The emission rate represents a key parameter that can be adopted to estimate exposure in typical indoor microenvironments through well-mixed models. To this end, we have estimated the overexposure to particle number concentration in a 40-m^3 office due to a 1-hour 3D printing activity. The simulations of particle number concentration were carried out considering the different filaments under investigation at the extrusion temperature suggested by the manufacturer, both in open and closed printing chamber configurations. The 1-hour average particle number concentration (C_{avg}) was calculated considering zero concentration at the beginning of the printing activity as:

$$C_{avg} = \frac{ER}{(AER + k) \cdot V} \cdot \left(1 - \frac{1}{(AER + k) \cdot T} \left(1 - e^{-(AER+k) \cdot T} \right) \right) \quad (2)$$

where the volume V is 40 m^3, the averaging time T is 1 hour, and the deposition rate k is 0.7 h^{-1} [63]. Simulations were performed by varying the AER from 0.2 h^{-1}, a value characteristic of a naturally-ventilated confined space [59], to 8 h^{-1}. The 1-h average concentrations were then compared to the guideline value suggested by the World Health Organization (WHO) as high particle number concentration [64], i.e., 2 × 10^4 part. cm^{-3}. The authors point out that the exposure to particle number concentrations in indoor environments is not regulated; thus, the guideline value suggested by the WHO represents the only attempt to define whether the exposure can be considered high or not.

3. Results and discussions

3.1. Emission rate data

Fig. 2 illustrates particle number and PM_{10} concentration trends obtained during one of the tests with the PP filament at different printing temperatures in both open and closed printing chamber configurations.

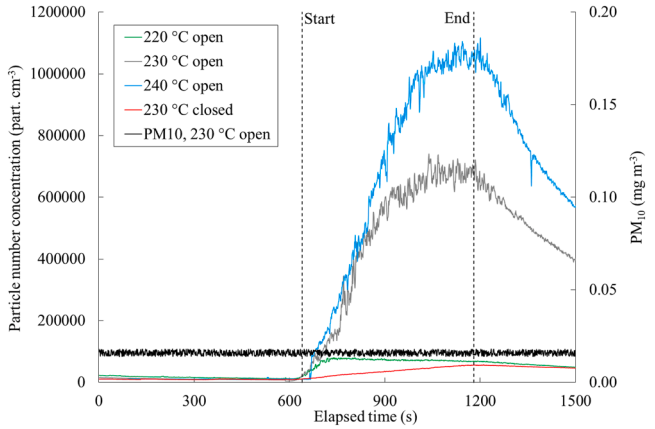

Fig. 2. Trends of particle number and PM_{10} concentrations obtained from the tests carried out at different temperatures (220, 230, 240 °C) and various printing chamber configurations (open, closed) using the PP filament. The trends represent one of the five tests carried out for each test condition.

After a 10-minute background concentration measurement, the trends show a rapid increase in particle number concentration shortly after the start of printing, followed by a decay in concentration as the extrusion ends. During the printing chamber's warm-up period, there is no change in particle number concentration; thus, all particles detected can be attributed solely to the printing process. The trends clearly show a higher concentration peak for higher extrusion temperatures, as reported in other studies for different filament materials [46,52,60]. When printing occurs in a closed printing chamber configuration, the peak concentration of particles is significantly lower compared to an open printing chamber configuration, likely due to the presence of the HEPA filter. Nonetheless, an increase in concentration is still detectable, demonstrating that some air leakages can occur when the printing chamber is closed. Finally, the trends of PM_{10} concentration obtained at 230 °C with the printing chamber open revealed a negligible emission in terms of particle mass (descriptive of super-micrometric particles), as we also previously showed for other filament materials [52]. Similar trends were obtained for the other PM metrics (PM_1 and $PM_{2.5}$) and all the filament materials under testing. Thus, the emission in terms of PMs is not further discussed in the paper.

The emission rates were estimated as described in Section 2.3, and the values are reported in Table 4 and Fig. 3a. The ERs evaluated for closed printing chamber configuration (average values ranging from 2.68×10^9 part. min^{-1} to 3.23×10^{10} part. min^{-1} at the extrusion temperature suggested by the manufacturers) resulted in an order of magnitude lower than those for open printing chamber configuration (average values ranging from 6.55×10^{10} part. min^{-1} to 1.07×10^{12} part. min^{-1} at the extrusion temperature suggested by the manufacturers), as established by the results of the statistical analysis,

Table 4
Summary of the estimated emission rates in terms of particle number and of the measured modes of the particle number distributions at the peak during the 3D printing for the different filaments analyzed at different extrusion temperatures, and different printing chamber configurations (open or closed). Average temperature and relative humidity data measured during the tests are also reported; they represent averages across replicates.

Filament material	Extrusion temperature (°C)	Printing chamber configuration	ER (part. min^{-1})	Mode of the particle number distribution at peak (nm)	Average temperature and relative humidity
TPE	220	open	$1.67 \pm 0.15 \times 10^{10}$	38 ± 2	22.2 °C, 48.9 %
	230	open	$8.17 \pm 0.90 \times 10^{10}$	37 ± 3	21.1 °C, 47.6 %
	240	open	$2.27 \pm 0.16 \times 10^{11}$	37 ± 2	23.2 °C, 48.0 %
	230	closed	$4.90 \pm 0.49 \times 10^{9}$	85 ± 4	20.9 °C, 50.3 %
TPU	220	open	$5.46 \pm 0.44 \times 10^{10}$	36 ± 3	22.8 °C, 46.6 %
	230	open	$9.61 \pm 0.95 \times 10^{10}$	38 ± 3	22.9 °C, 47.8 %
	240	open	$1.36 \pm 0.12 \times 10^{11}$	38 ± 3	21.6 °C, 49.8 %
	230	closed	$5.99 \pm 0.54 \times 10^{9}$	91 ± 5	22.3 °C, 48.1 %
TPU-CNT	220	open	$3.67 \pm 0.40 \times 10^{10}$	52 ± 4	23.5 °C, 47.8 %
	230	open	$6.55 \pm 0.62 \times 10^{10}$	28 ± 1	20.5 °C, 49.9 %
	240	open	$1.14 \pm 0.13 \times 10^{11}$	30 ± 2	21.3 °C, 47.9 %
	230	closed	$2.68 \pm 0.19 \times 10^{9}$	59 ± 4	21.1 °C, 46.4 %
PP	220	open	$1.70 \pm 0.19 \times 10^{11}$	55 ± 3	22.8 °C, 47.5 %
	230	open	$7.31 \pm 0.66 \times 10^{11}$	48 ± 2	20.5 °C, 46.3 %
	240	open	$1.01 \pm 0.08 \times 10^{12}$	40 ± 2	22.2 °C, 49.4 %
	230	closed	$3.23 \pm 0.23 \times 10^{10}$	76 ± 4	21.2 °C, 46.9 %
PC	235	open	$2.09 \pm 0.21 \times 10^{11}$	39 ± 3	23.2 °C, 48.1 %
	245	open	$1.07 \pm 0.12 \times 10^{12}$	28 ± 1	20.5 °C, 50.9 %
	255	open	$5.56 \pm 0.05 \times 10^{11}$	29 ± 2	22.2 °C, 48.9 %
	245	closed	$2.95 \pm 0.30 \times 10^{10}$	49 ± 2	21.1 °C, 47.6 %

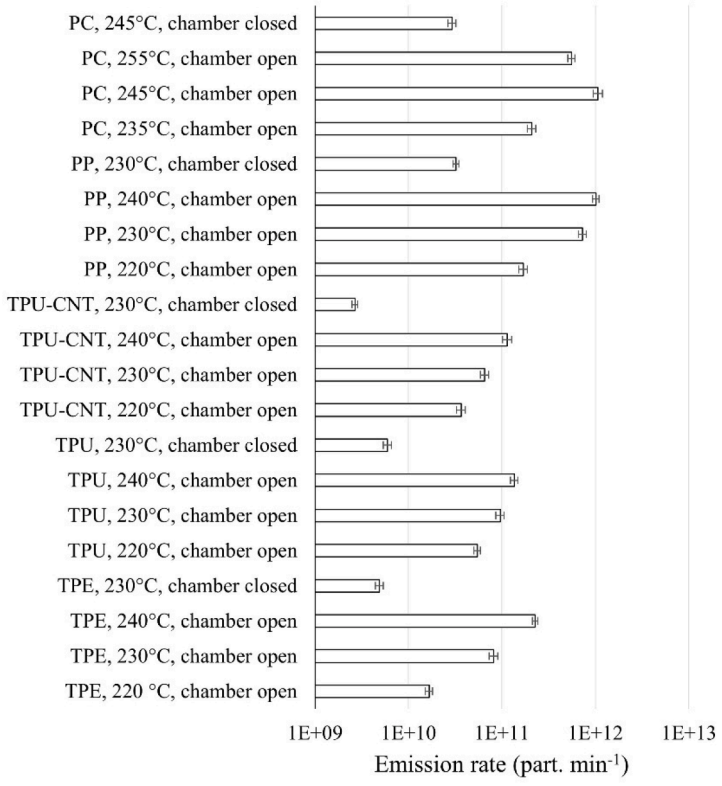

a)

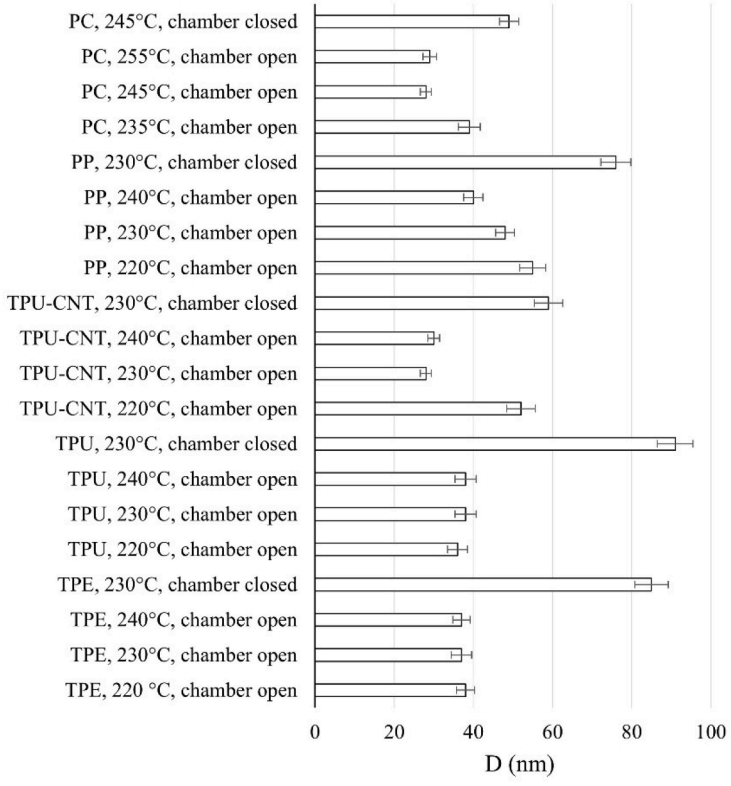

b)

Fig. 3. Average particle number emission rates (a) and modes of size distribution at the peak (b) as a function of the extrusion temperature during the 3D printing for the different filaments analyzed at different extrusion temperatures, and different printing chamber configurations (open or closed). Error bars represent standard deviations.

specifically the parametric test (ANOVA test) and the subsequent post-hoc test (Tukey-Kramer test). This confirms the effect of the printing chamber and the HEPA filter in reducing the particle number emission of the 3D printing activity. Moreover, except for PC filament, the ERs monotonically increased with the extrusion temperatures; in particular, statistical analysis confirmed that for a given material, variations in extrusion temperature result in statistically significant changes in emission. This phenomenon was already observed and reported in previous works [46,52,60] and could be related to the decomposition phenomena occurring at the filament materials, which are more intense as the temperature increases [65–67]. Indeed, higher extrusion temperatures can increase the vapor pressure of organic materials, potentially facilitating the particle formation process [68,69].

The estimated average emission rates of TPE (4.90×10^9 - 2.27×10^{11} part. min^{-1}), TPU (5.99×10^9 - 1.36×10^{11} part. min^{-1}), and TPU-CNT (2.68×10^9 - 1.14×10^{11} part. min^{-1}) are lower than those for PP (3.23×10^{10} - 1.01×10^{12} part. min^{-1}) and PC (2.95×10^{10} - 1.07×10^{12} part. min^{-1}) as obtained from the statistical analysis (ANOVA and Tukey-Kramer test). The elevated emissions observed in polycarbonate (PC) may be attributed to its higher printing temperatures, whereas further evaluation should be carried out to understand the high emissions of polypropylene filaments. The standard deviation of the emission rates, reported in Table 4, ranges from 7 % to 11 %, indicating good repeatability of the tests.

Proper comparisons with existing literature values are hardly possible. Indeed, the various studies employed different measurement protocols, including sampling site and instrumentation [38]. For a clearer comparison, we note that most studies investigating emission rates related to 3D printing primarily examined ABS and PLA filaments. These investigations reported emission rates ranging from 2.4×10^8 to 1.8×10^{11} part. min^{-1} for ABS, and from 4.9×10^8 to 2.8×10^{12} part. min^{-1} for PLA [29–31,33,39,46,47,52]. Other studies have analyzed TPU filaments [45,51] and PP filaments [51] without reporting emission rates, whereas Azimi et al. reported an ER of 2×10^{10} part. min^{-1} for a variant of TPE (nylon-TPE) printed at 235 °C with a printer with a plexiglass printing chamber [47].

3.2. Particle distribution data

In Fig. 4, illustrative examples of particle number distributions measured through the SMPS 3936 are reported. In particular, Fig. 4a shows the particle number distribution evolution measured for one test during printing in the open printing chamber configuration for the PP filament at an extrusion temperature of 230 °C. The particle number distribution evolution displays that, starting from a unimodal background distribution with a mode at about 100 nm (typical of aged aerosol), during the printing activity, the emission of freshly-generated particles occurs, leading to a unimodal particle size distribution with a mode of about 50 nm at the concentration peak (at t = 20 min). During the particle concentration decay period, a negligible increase in the particle size distribution mode was observed; no significant coagulation phenomena were detected during this period. Therefore, ERs can be appropriately calculated using the model reported in Section 2.3 (eq. (1)). Similar behaviors were identified for all the materials and tests performed, thus confirming the applicability of the aforementioned emission rate model.

For all the tests performed, a unimodal distribution was detected (similar to that reported in Fig. 4), thus, for the sake of brevity, in Table 4 and Fig. 3b, the particle distribution modes for all the tests are summarized: in the case of open printing chamber configuration, the modes ranged from <30 nm to >50 nm. Compared to existing literature [30,31,33–35,45], the emission modes align closely with those previously reported, even if some studies [34,36,37,51] observed smaller diameter modes. This data variability found in the literature could be due to the different influence parameters affecting the emission (chemical composition of the material, extrusion temperature, etc.). Indeed, the extrusion temperature has a visible effect on the mode of the emitted particles. For TPE and TPU, a very similar average mode (36–38 nm) was measured regardless of the extrusion temperature, on the contrary, for TPU-CNT, PP, and PC, the mode shifted towards lower diameters for higher extrusion temperatures: this may be because, as the extrusion temperature rises, polymers experience more intense pyrolysis, generating more volatile organic compounds (VOCs), fragmented polymer chains, and aromatic compounds, then condensing spontaneously, forming ultrafine particles [47,70].

Fig. 4b shows the particle number distribution evolution measured during printing activity in the closed printing chamber configuration for the PP filament at an extrusion temperature of 230 °C. After the background period (with an aged aerosol characterized by a mode of about 100 nm), concentration increases, and a unimodal distribution (with a mode of 76 nm) was detected at the concentration peak. Then, during the concentration decay, the mode remains almost constant. Thus, the mode measured for the closed printing chamber configuration was larger than for the open printing chamber at the same extrusion temperature. This condition was recognized for all the investigated materials, as summarized in Table 4 and Fig. 3b: the average modes for closed printing chamber configuration ranged from 49 nm (for PP) to 91 nm (for TPU). The reason for such higher modes occurring in closed printing chamber tests is likely due to the coagulation phenomena occurring in the printing chamber. Indeed, the high emission of particles will cause very high particle concentrations in the small printing chamber, such that particles will quickly coagulate due to the small volume available, then reducing the concentration and increasing the modes: indeed, as soon as the particles are emitted they present a mode similar to the open printing chamber configuration (e.g., 48 nm for PP), nonetheless, due to the rapid coagulation such mode suddenly increases (e.g., 76 nm for PP). Thus, the particle distribution of the particles exfiltrating the printing chamber will present a distribution that has already undergone a coagulation process. In the case of small measurement chamber dimensions for different filament materials, such coagulation phenomena were already observed in other studies [30,31,33,34,36,38,42,48,49].

3.3. Exposure in a real-world scenario

In Fig. 5, the 1-hour average concentrations (C_{avg} in eq. (2)) due to the 3D printing activity in a 40-m^3 office with a zero concentration at the beginning of the phenomenon were reported as a function of the AER and of the average emission rate values, for the exposure scenario defined in Section 2.4. The trends show that scenarios with no printing chamber (i.e., printing chamber open) and reduced air exchange rates (e.g., naturally ventilated environment) result in 1-hour average concentrations much larger than the guideline values suggested by the WHO. In particular, for highly emitting filaments (PC and PP), $C_{avg} > 1 \times 10^5$ part. cm^{-3} were obtained even for an AER of 8 h^{-1}. For TPE, TPU, and TPU-CNT, characterized by lower emission rates, mechanical ventilation (AER > 2 h^{-1}) is required to ensure average concentrations remain within the WHO guideline value.

Nonetheless, when printing activities are conducted with the printing chamber closed (equipped with a HEPA filter), the resulting 1-hour average concentrations in the office are lower than the WHO guideline values, regardless of the room ventilation. Thus, a closed printing chamber with a HEPA filter represents an effective environmental control measure for limiting exposure in enclosed spaces where 3D printing is performed.

Summarizing, for the very first time, we quantified the emission of airborne particles from 3D printing using thermoplastic polymeric materials. This represents a novel contribution to scientific literature. Future studies should focus on evaluating the toxicity of the emitted particles. To this end, airborne particle samplings should be carried out, and consequent chemical analysis of the collected particles should be conducted to evaluate the possible presence of toxic compounds (e.g., PAHs and heavy metals) as we did in previous papers [2,71].

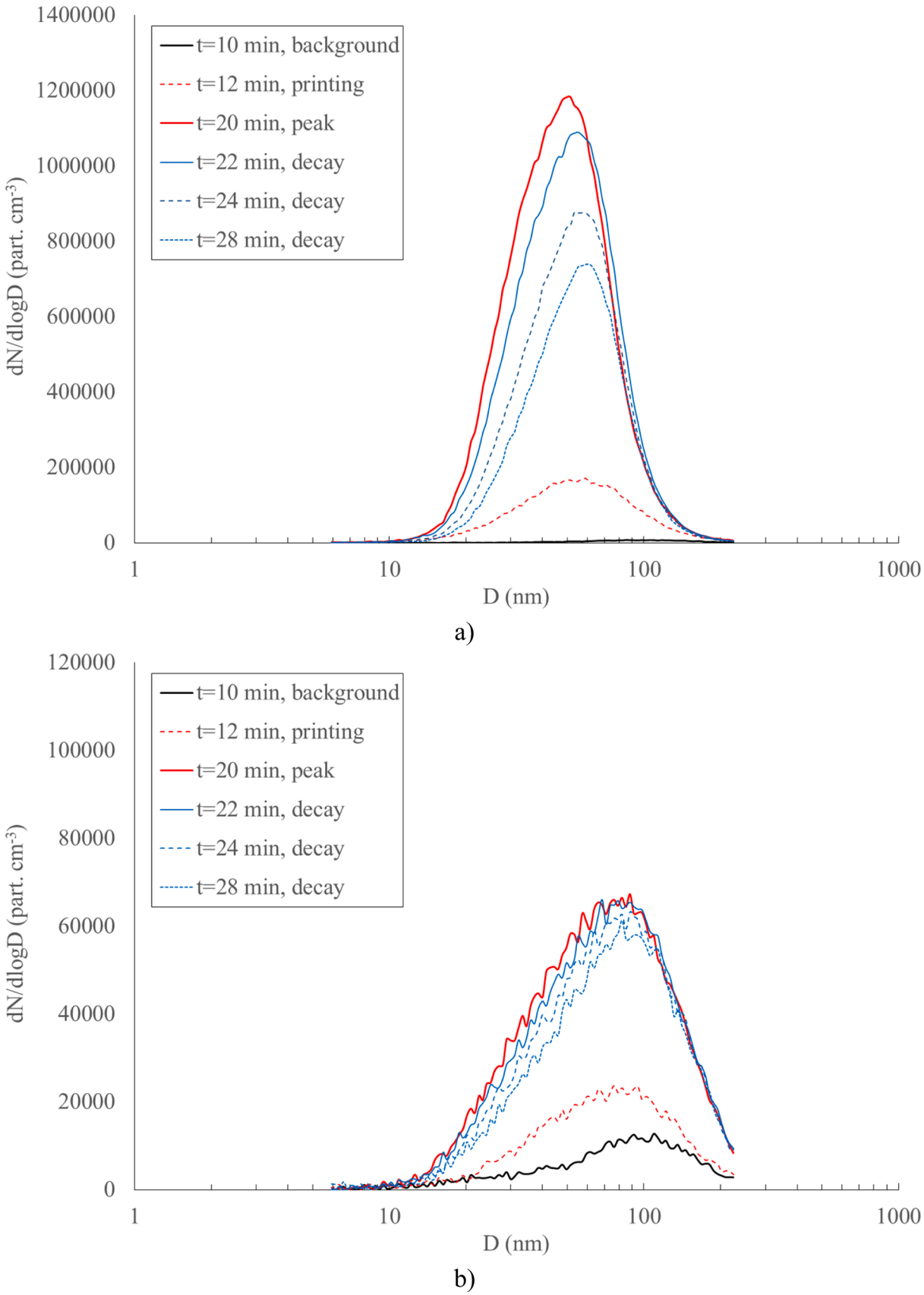

Fig. 4. Particle number distribution evolution during printing in the open printing chamber configuration (a) and in the closed printing chamber configuration (b) for the PP filament at an extrusion temperature of 230 °C. The distribution evolution represents one of the five tests carried out for each test condition.

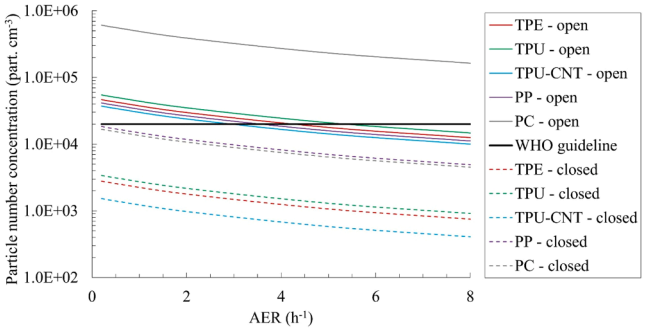

Fig. 5. Trends of 1-hour average particle number concentrations (C_{avg}), calculated for average emission rate values, as a function of the AER and the filament material for the exposure scenario investigated: 3D printing activity of 1 hour in a 40-m^3 office with a zero concentration at the beginning of the phenomenon.

4. Conclusions

This study analyzed particle emissions from a 3D printer using thermoplastic materials: thermoplastic polyurethane, carbon-nanotube-enhanced thermoplastic polyurethane, thermoplastic elastomer, polypropylene, and polycarbonate. Tests covered different extrusion temperatures and two chamber configurations, open and closed with a HEPA filter, while continuously monitoring particle number concentrations, PM fractions, and size distributions. Emission rates were calculated for all conditions.

Emissions were dominated by sub-micrometric particles, with negligible changes in mass concentrations. Open-chamber emission rates (6.55×10^{10} – 1.07×10^{12} part. min^{-1}) were about one order of magnitude higher than those from closed chambers with HEPA filters (2.68×10^{9} – 3.23×10^{10} part. min^{-1}), confirming the filter's effectiveness. Polypropylene and polycarbonate showed the highest emissions (up to 1×10^{12} part. min^{-1} in open chambers).

Emission rates generally increased with extrusion temperature, likely due to enhanced thermal decomposition of the filaments. In open chambers, particle size modes ranged from <30 nm to >50 nm and shifted to smaller diameters at higher temperatures. Closed-chamber tests yielded larger modes (49–91 nm), consistent with particle coagulation in the confined space.

Exposure modeling for a 40 m^3 office showed that printing without a chamber could produce hazardous concentrations, especially with polypropylene and polycarbonate, exceeding 1×10^{5} part. cm^{-3} even at high ventilation rates (8 h^{-1}). For other filaments, WHO guideline values (2×10^{4} part. cm^{-3}) could only be met with ventilation >2 h^{-1}. Using a closed chamber with a HEPA filter consistently reduced concentrations below WHO limits for all filaments and ventilation conditions, highlighting its effectiveness as an exposure control measure in enclosed spaces.

Data availability

Data will be made available on request.

Funding

This research received no specific grant from any funding agency in the public, commercial, or not-for-profit sectors.

CRediT authorship contribution statement

L. Fappiano: Writing – original draft, Validation, Investigation. **E. Caracci:** Writing – review & editing, Validation, Investigation. **A. Ceccacci:** Writing – original draft, Investigation. **G. Iannitti:** Supervision. **G. Buonanno:** Writing – review & editing, Supervision, Conceptualization. **L. Stabile:** Writing – review & editing, Writing – original draft, Validation, Supervision, Conceptualization.

Declaration of competing interest

The authors declare that they have no known competing financial interests or personal relationships that could have appeared to influence the work reported in this paper.

References

[1] L. Morawska, A. Afshari, G.N. Bae, G. Buonanno, C.Y.H. Chao, O. Hänninen, W. Hofmann, C. Isaxon, E.R. Jayaratne, P. Pasanen, T. Salthammer, M. Waring, A. Wierzbicka, Indoor aerosols: from personal exposure to risk assessment, Indoor. Air. 23 (2013) 462–487, https://doi.org/10.1111/ina.12044.

[2] L. Fappiano, E. Caracci, A. Iannone, A. Murru, P. Avino, M. Campagna, G. Buonanno, L. Stabile, Emission rates of particle-bound heavy metals and polycyclic aromatic hydrocarbons in PM fractions from indoor combustion sources, Build. Env. 265 (2024) 112033, https://doi.org/10.1016/j.buildenv.2024.112033.

[3] E. Caracci, L. Canale, G. Buonanno, L. Stabile, Effectiveness of eco-feedback in improving the indoor air quality in residential buildings: mitigation of the exposure to airborne particles, Build. Env. 226 (2022) 109706, https://doi.org/10.1016/j.buildenv.2022.109706.

[4] G. Buonanno, L. Morawska, L. Stabile, Particle emission factors during cooking activities, Atmos. Env. 43 (2009) 3235–3242, https://doi.org/10.1016/j.atmosenv.2009.03.044.

[5] G. Buonanno, G. Johnson, L. Morawska, L. Stabile, Volatility characterization of cooking-generated aerosol particles, Aerosol. Sci. Technol. 45 (2011) 1069–1077, https://doi.org/10.1080/02786826.2011.580797.

[6] L. Stabile, E.R. Jayaratne, G. Buonanno, L. Morawska, Charged particles and cluster ions produced during cooking activities, Sci. Total. Environ 497–498 (2014) 516–526, https://doi.org/10.1016/j.scitotenv.2014.08.011.

[7] L. Stabile, F.C. Fuoco, S. Marini, G. Buonanno, Effects of the exposure to indoor cooking-generated particles on nitric oxide exhaled by women, Atmos. Env. 103 (2015) 238–246, https://doi.org/10.1016/j.atmosenv.2014.12.049.

[8] L.A. Wallace, S.J. Emmerich, C. Howard-Reed, Source strengths of ultrafine and fine particles due to cooking with a gas stove, Env. Sci. Technol. 38 (2004) 2304–2311, https://doi.org/10.1021/es0306260.

[9] R. Tang, C. Pfrang, Indoor particulate matter (PM) from cooking in UK students' studio flats and associated intervention strategies: evaluation of cooking methods, PM concentrations and personal exposures using low-cost sensors, Env. Sci. 3 (2023) 537–551, https://doi.org/10.1039/D2EA00171C.

[10] S. Ma, W. Liu, C. Meng, J. Dong, S. Zhang, Temperature-dependent particle mass emission rate during heating of edible oils and their regression models, Environ. Pollut. 323 (2023) 121221, https://doi.org/10.1016/j.envpol.2023.121221.

[11] L. Stabile, F.C. Fuoco, G. Buonanno, Characteristics of particles and black carbon emitted by combustion of incenses, candles and anti-mosquito products, Build. Env. 56 (2012) 184–191, https://doi.org/10.1016/j.buildenv.2012.03.005.

[12] M.P. Spilak, M. Frederiksen, B. Kolarik, L. Gunnarsen, Exposure to ultrafine particles in relation to indoor events and dwelling characteristics, Build. Env. 74 (2014) 65–74, https://doi.org/10.1016/j.buildenv.2014.01.007.

[13] S.W. See, R. Balasubramanian, Characterization of fine particle emissions from incense burning, Build. Env. 46 (2011) 1074–1080, https://doi.org/10.1016/j.buildenv.2010.11.006.

[14] Y. Kim, A. Gidwani, B.E. Wyslouzil, C.W. Sohn, Source term models for fine particle resuspension from indoor surfaces, Build. Env. 45 (2010) 1854–1865, https://doi.org/10.1016/j.buildenv.2010.02.016.

[15] Y. Ishizuka, M. Tokumura, A. Mizukoshi, M. Noguchi, Y. Yanagisawa, Measurement of secondary products during oxidation reactions of terpenes and ozone based on the PTR-MS analysis: effects of coexistent carbonyl compounds, Int. J. Env. Res. Public. Health 7 (2010) 3853–3870, https://doi.org/10.3390/ijerph7113853.

[16] F.C. Fuoco, L. Stabile, G. Buonanno, C.V. Trassiera, A. Massimo, A. Russi, M. Mazaheri, L. Morawska, A. Andrade, Indoor air quality in naturally ventilated Italian classrooms, Atmosphere 6 (2015) 1652–1675, https://doi.org/10.3390/atmos6111652.

[17] R.L. Corsi, J.A. Siegel, C. Chiang, Particle resuspension during the use of vacuum cleaners on residential carpet, J. Occup. Env. Hyg. 5 (2008) 232–238, https://doi.org/10.1080/15459620801901165.

[18] H.-C. Chuang, T. Jones, K. BéruBé, Combustion particles emitted during church services: implications for human respiratory health, Env. Int. 40 (2012) 137–142, https://doi.org/10.1016/j.envint.2011.07.009.

[19] G. Buonanno, F.C. Fuoco, S. Marini, L. Stabile, Particle resuspension in school gyms during physical activities, Aerosol. Air. Qual. Res. 12 (2012), https://doi.org/10.4209/aaqr.2011.11.0209.

[20] T. Wu, T. Müller, N. Wang, J. Byron, S. Langer, J. Williams, D. Licina, Indoor emission, oxidation, and new particle formation of personal care product related volatile organic compounds, Env. Sci. Technol. Lett. 11 (2024) 1053–1061, https://doi.org/10.1021/acs.estlett.4c00353.

[21] L. Fontana, L. Fappiano, L. Stabile, A. Chaillon, G. Buonanno, Chlorine gas and ultrafine particle emissions from bleach disinfection: exposure risk

characterization, J. Occup. Med. Toxicol. 20 (2025) 18, https://doi.org/10.1186/s12995-025-00465-6.
[22] T. Schripp, M. Wensing, E. Uhde, T. Salthammer, C. He, L. Morawska, Evaluation of ultrafine particle emissions from laser printers using emission test chambers, Env. Sci. Technol. 42 (2008) 4338–4343, https://doi.org/10.1021/es702426m.
[23] C.-W. Lee, D.-J. Hsu, Measurements of fine and ultrafine particles formation in photocopy centers in Taiwan, Atmos. Env. 41 (2007) 6598–6609, https://doi.org/10.1016/j.atmosenv.2007.04.016.
[24] H. Destaillats, R.L. Maddalena, B.C. Singer, A.T. Hodgson, T.E. McKone, Indoor pollutants emitted by office equipment: a review of reported data and information needs, Atmos. Env. 42 (2008) 1371–1388, https://doi.org/10.1016/j.atmosenv.2007.10.080.
[25] T.D. Ngo, A. Kashani, G. Imbalzano, K.T.Q. Nguyen, D. Hui, Additive manufacturing (3D printing): a review of materials, methods, applications and challenges, Compos. B 143 (2018) 172–196, https://doi.org/10.1016/j.compositesb.2018.02.012.
[26] M. Jayakrishna, M. Vijay, B. Khan, An overview of extensive analysis of 3D printing applications in the manufacturing sector, J. Eng. 2023 (2023) 1–23, https://doi.org/10.1155/2023/7465737.
[27] W.C. Hill, A. Korchevskiy, The size distribution of nanoparticles emitted from advanced manufacturing devices impacts predicted carcinogenic potential, Front. Public. Health (2025). Volume 13-2025, https://www.frontiersin.org/journals/public-health/articles/10.3389/fpubh.2025.1582690.
[28] Y. Deng, S.-J. Cao, A. Chen, Y. Guo, The impact of manufacturing parameters on submicron particle emissions from a desktop 3D printer in the perspective of emission reduction, Build. Env. 104 (2016) 311–319, https://doi.org/10.1016/j.buildenv.2016.05.021.
[29] P. Steinle, Characterization of emissions from a desktop 3D printer and indoor air measurements in office settings, J. Occup. Env. Hyg. 13 (2016) 121–132, https://doi.org/10.1080/15459624.2015.1091957.
[30] J. Yi, Ryan F. LeBouf, Matthew G. Duling, Timothy Nurkiewicz, Bean T. Chen, Diane Schwegler-Berry, M.Abbas Virji, B. A, Stefaniak, Emission of particulate matter from a desktop three-dimensional (3D) printer, J. Toxicol. Environ. Health. A 79 (2016) 453–465, https://doi.org/10.1080/15287394.2016.1166467.
[31] B. Stephens, P. Azimi, Z. El Orch, T. Ramos, Ultrafine particle emissions from desktop 3D printers, Atmos. Env. 79 (2013) 334–339, https://doi.org/10.1016/j.atmosenv.2013.06.050.
[32] I. Gümperlein, E. Fischer, G. Dietrich-Gümperlein, S. Karrasch, D. Nowak, R. A. Jörres, R. Schierl, Acute health effects of desktop 3D printing (fused deposition modeling) using acrylonitrile butadiene styrene and polylactic acid materials: an experimental exposure study in human volunteers, Indoor. Air 28 (2018) 611–623, https://doi.org/10.1111/ina.12458.
[33] Y. Kim, C. Yoon, S. Ham, J. Park, S. Kim, O. Kwon, P.-J. Tsai, Emissions of nanoparticles and gaseous material from 3D printer operation, Env. Sci. Technol. 49 (2015) 12044–12053, https://doi.org/10.1021/acs.est.5b02805.
[34] M.E. Vance, V. Pegues, S. Van Montfrans, W. Leng, L.C. Marr, Aerosol emissions from fuse-deposition modeling 3D printers in a chamber and in real indoor environments, Env. Sci. Technol. 51 (2017) 9516–9523, https://doi.org/10.1021/acs.est.7b01546.
[35] M.T. Farcas, Walter McKinney, Chaolong Qi, Kyle W. Mandler, Lori Battelli, Sherri A. Friend, Aleksandr B. Stefaniak, Mark Jackson, Marlene Orandle, Ava Winn, Michael Kashon, Ryan F. LeBouf, Kristen A. Russ, Duane R. Hammond, Dru Burns, Anand Ranpara, Treye A. Thomas, Joanna Matheson, Y, Qian, Pulmonary and systemic toxicity in rats following inhalation exposure of 3-D printer emissions from acrylonitrile butadiene styrene (ABS) filament, Inhal. Toxicol. 32 (2020) 403–418, https://doi.org/10.1080/08958378.2020.1834034.
[36] L. Mendes, A. Kangas, K. Kukko, B. Mølgaard, A. Säämänen, T. Kanerva, I. Flores Ituarte, M. Huhtiniemi, H. Stockmann-Juvala, J. Partanen, K. Hämeri, K. Eleftheriadis, A.-K. Viitanen, Characterization of emissions from a desktop 3D printer, J. Ind. Ecol. 21 (2017) S94–S106, https://doi.org/10.1111/jiec.12569.
[37] T.L. Zontek, B.R. Ogle, J.T. Jankovic, S.M. Hollenbeck, An exposure assessment of desktop 3D printing, J. Chem. Health. Saf. 24 (2017) 15–25, https://doi.org/10.1016/j.jchas.2016.05.008.
[38] J. Zhang, D.-R. Chen, S.-C. Chen, Sampling and characterization of particle emission from the 3D FDM printing, J. Build. Eng. 52 (2022) 104476, https://doi.org/10.1016/j.jobe.2022.104476.
[39] O. Kwon, C. Yoon, S. Ham, J. Park, J. Lee, D. Yoo, Y. Kim, Characterization and control of nanoparticle emission during 3D printing, Env. Sci. Technol. 51 (2017) 10357–10368, https://doi.org/10.1021/acs.est.7b01454.
[40] D.A. Baguley, G.S. Evans, D. Bard, P.S. Monks, R.L. Cordell, Review of volatile organic compound (VOC) emissions from desktop 3D printers and associated health implications, J. Expo. Sci. Env. Epidemiol. (2025), https://doi.org/10.1038/s41370-025-00778-y.
[41] J. Zhang, D.-R. Chen, S.-C. Chen, A review of emission characteristics and control strategies for particles emitted from 3D fused deposition modeling (FDM) printing, Build. Env. 221 (2022) 109348, https://doi.org/10.1016/j.buildenv.2022.109348.
[42] L. Barnett, Q. Zhang, S. Sharma, S. Alqahtani, J. Shannahan, M. Black, C. Wright, 3D printer emissions elicit filament-specific and dose-dependent metabolic and genotoxic effects in human airway epithelial cells, Front. Public. Health. 12 (2024) 1408842, https://doi.org/10.3389/fpubh.2024.1408842.
[43] G. Felici, J.I. Lachowicz, S. Milia, E. Cannizzaro, L. Cirrincione, T. Congiu, M. Jaremko, M. Campagna, L.I. Lecca, A pilot study of occupational exposure to ultrafine particles during 3D printing in research laboratories, Front. Public. Health. 11 (2023) 1144475, https://doi.org/10.3389/fpubh.2023.1144475.
[44] Q. Zhang, M. Wilson, M.S. Black, Impact of 3D printing on indoor particulate matter and volatile organic compounds in educational environments, Build. Env. 282 (2025) 113324, https://doi.org/10.1016/j.buildenv.2025.113324.
[45] R. Chýlek, L. Kudela, J. Pospíšil, L. Šnajdárek, Parameters influencing the emission of ultrafine particles during 3D printing, Int. J. Env. Res. Public. Health 18 (2021) 11670, https://doi.org/10.3390/ijerph182111670.
[46] Q. Zhang, J.P.S. Wong, A.Y. Davis, M.S. Black, R.J. Weber, Characterization of particle emissions from consumer fused deposition modeling 3D printers, Aerosol. Sci. Technol. 51 (2017) 1275–1286, https://doi.org/10.1080/02786826.2017.1342029.
[47] P. Azimi, D. Zhao, C. Pouzet, N.E. Crain, B. Stephens, Emissions of ultrafine particles and volatile organic compounds from commercially available desktop three-dimensional printers with multiple Filaments, Env. Sci. Technol. 50 (2016) 1260–1268, https://doi.org/10.1021/acs.est.5b04983.
[48] E.L. Floyd, Jun Wang, L. J, Regens, Fume emissions from a low-cost 3-D printer with various filaments, J. Occup. Env. Hyg. 14 (2017) 523–533, https://doi.org/10.1080/15459624.2017.1302587.
[49] M. Poikkimäki, V. Koljonen, N. Leskinen, M. Närhi, O. Kangasniemi, O. Kausiala, M. Dal Maso, Nanocluster aerosol emissions of a 3D printer, Env. Sci. Technol. 53 (2019) 13618–13628, https://doi.org/10.1021/acs.est.9b05317.
[50] H. Jeon, J. Park, S. Kim, K. Park, C. Yoon, Effect of nozzle temperature on the emission rate of ultrafine particles during 3D printing, Indoor. Air. 30 (2020) 306–314, https://doi.org/10.1111/ina.12624.
[51] H. Garcia-Gonzalez, M.T. Lopez-Pola, Unlocking the nanoparticle emission potential: a study of varied filaments in 3D printing, Env. Sci. Pollut. Res. 31 (2024) 31188–31200, https://doi.org/10.1007/s11356-024-33257-2.
[52] L. Stabile, M. Scungio, G. Buonanno, F. Arpino, G. Ficco, Airborne particle emission of a commercial 3D printer: the effect of filament material and printing temperature, Indoor. Air 27 (2017) 398–408, https://doi.org/10.1111/ina.12310.
[53] H. Romanowski, F.S. Bierkandt, A. Luch, P. Laux, Summary and derived risk assessment of 3D printing emission studies, Atmos. Env. 294 (2023) 119501, https://doi.org/10.1016/j.atmosenv.2022.119501.
[54] S. Cui, M. Cohen, P. Stabat, D. Marchio, CO2 tracer gas concentration decay method for measuring air change rate, Build. Env. 84 (2015) 162–169, https://doi.org/10.1016/j.buildenv.2014.11.007.
[55] P. Jagadeesh, S. Mavinkere Rangappa, S. Siengchin, M. Puttegowda, S.M. K. Thiagamani, G. R, M. Hemath Kumar, O.P. Oladijo, V. Fiore, M.M. Moure Cuadrado, Sustainable recycling technologies for thermoplastic polymers and their composites: a review of the state of the art, Polym. Compos. 43 (2022) 5831–5862, https://doi.org/10.1002/pc.27000.
[56] S. Ricci, A. Pagano, A. Ceccacci, G. Iannitti, N. Bonora, An investigation of the monotonic and cyclic behavior of additively manufactured TPU, Eng. Proc 85 (2025), https://doi.org/10.3390/engproc2025085018.
[57] M.E. Grigore, Methods of recycling, properties and applications of recycled thermoplastic polymers, Recycling 2 (2017), https://doi.org/10.3390/recycling2040024.
[58] P. Schewe, A. Roehler, S. Spintzyk, F. Huettig, Shock absorption behavior of elastic polymers for sports mouthguards: an In vitro comparison of thermoplastic forming and additive manufacturing, Materials 15 (2022), https://doi.org/10.3390/ma15082928.
[59] S. Boria, A. Scattina, Energy absorption capability of laminated plates made of fully thermoplastic composite, Proc. Inst. Mech. Eng. C 232 (2018) 1389–1401, https://doi.org/10.1177/0954406218760059.
[60] A.B. Stefaniak, R.F. LeBouf, J. Yi, J. Ham, T. Nurkewicz, D.E. Schwegler-Berry, B. T. Chen, J.R. Wells, M.G. Duling, R.B. Lawrence, S.B. Martin Jr., A.R. Johnson, M. A. Virji, Characterization of chemical contaminants generated by a desktop fused deposition modeling 3-dimensional printer, J. Occup. Env. Hyg. 14 (2017) 540–550, https://doi.org/10.1080/15459624.2017.1302589.
[61] C. He, L. Morawska, J. Hitchins, D. Gilbert, Contribution from indoor sources to particle number and mass concentrations in residential houses, Atmos. Env. 38 (2004) 3405–3415, https://doi.org/10.1016/j.atmosenv.2004.03.027.
[62] W.C. Driscoll, Robustness of the ANOVA and Tukey-Kramer statistical tests, Comput. Ind. Eng. 31 (1996) 265–268, https://doi.org/10.1016/0360-8352(96)00127-1.
[63] L.A. Wallace, S.J. Emmerich, C. Howard-Reed, Effect of central fans and in-duct filters on deposition rates of ultrafine and fine particles in an occupied townhouse, Atmos. Env. 38 (2004) 405–413, https://doi.org/10.1016/j.atmosenv.2003.10.003.
[64] World Health Organization, WHO's global air-quality guidelines. Particulate matter (PM2.5 and PM10), ozone, nitrogen dioxide, sulfur dioxide and carbon monoxide, (2021).
[65] R. Al-Itry, K. Lamnawar, A. Maazouz, Improvement of thermal stability, rheological and mechanical properties of PLA, PBAT and their blends by reactive extrusion with functionalized epoxy, Polym. Degrad. Stab.97 (10) 1898–1914. https://doi.org/10.1016/j.polymdegradstab.2012.06.028.
[66] M.R. Mitchell, R.E. Link, M.-H. Yang, Y.-H. Lin, Measurement and simulation of thermal stability of poly(Lactic Acid) by thermogravimetric analysis, J. Test. Eval 37 (2009) 102271, https://doi.org/10.1520/jte102271.
[67] M.H. Yang, Y.H. Lin, Measurement and simulation of thermal stability of poly (Lactic Acid) by thermogravimetric analysis, J. Test. Eval. 37 (2009). http://www.scopus.com/inward/record.url?eid=2-s2.0-0042466444&partnerID=40&md5=2c32872a6f2873d9bbb9fc3209da6c07.
[68] D.J. Jarmer, C.S. Lengsfeld, T.W. Randolph, Nucleation and growth rates of poly(L-lactic acid) microparticles during precipitation with a compressed-fluid antisolvent, Langmuir. 2F:. ACS. J. Surf. Colloids. 20 (2004) 7254–7264, https://doi.org/10.1021/la049912v.

[69] J. Yang, Y. Zhang, S. Zheng, L. Huang, F. Chen, P. Fan, M. Zhong, Probing structure–heterogeneous nucleation efficiency relationship of mesoporous particles in polylactic acid microcellular foaming by supercritical carbon dioxide, J. Supercrit. Fluids.95 (11) 228–235. https://doi.org/10.1016/j.supflu.2014.08.020.
[70] J. Yi, Ryan F. LeBouf, Matthew G. Duling, Timothy Nurkiewicz, Bean T. Chen, Diane Schwegler-Berry, M.Abbas Virji, B. A, Stefaniak, Emission of particulate matter from a desktop three-dimensional (3D) printer, J. Toxicol. Environ. Health. A 79 (2016) 453–465, https://doi.org/10.1080/15287394.2016.1166467.
[71] E. Caracci, A. Iannone, F. Carriera, I. Notardonato, S. Pili, A. Murru, P. Avino, M. Campagna, G. Buonanno, L. Stabile, Size-segregated content of heavy metals and polycyclic aromatic hydrocarbons in airborne particles emitted by indoor sources, Sci. Rep. 14 (2024), https://doi.org/10.1038/s41598-024-70978-3.